Comparison of Cu_xS Films Grown by Atomic Layer Deposition and Chemical Vapor Deposition

Liesbeth Reijnen,* Ben Meester, Frits de Lange, Joop Schoonman, and Albert Goossens

Laboratory for Inorganic Chemistry, Delft University of Technology, Julianalaan 136,
2628 BL Delft, The Netherlands

Received November 28, 2003. Revised Manuscript Received March 8, 2005

Thin films of Cu_xS are deposited by both chemical vapor deposition (CVD) and atomic layer deposition (ALD) using copper bis-tetramethylheptanedionate, $Cu(thd)_2$, and H_2S as the precursors. Single-phase CuS and $Cu_{1.8}S$ can be deposited using both techniques, while in CVD also mixed phases can be formed. Comparing the ALD process with the CVD process leads to a better understanding of the reaction chemistry of both processes. The main factor is the decomposition of $Cu(thd)_2$ at 175 °C, which leads to a phase transition from CuS to $Cu_{1.8}S$ in ALD and deposition of mixed phases in CVD. Consequently, the phase transition is sharp in ALD and gradual in CVD. At temperatures higher than 250 °C, decomposition of $Cu(thd)_2$ occurs in the gas phase, leading to a transition from a reaction-limited regime to a thermodynamic regime in CVD and to loss of uniformity and homogeneity in ALD.

Introduction

The concept of nanostructured heterojunctions has been applied in dye-sensitized solar cells,[1] in solid-state solar cells,[2−5] and in so-called extremely thin absorber (ETA) solar cells.[6−8] The enhanced surface area in these heterojunctions ensures optimal light absorption close to the active p−n junction area, which allows a significant reduction of the minority carrier diffusion length. In most cases, optically transparent anatase TiO_2 is used as a nanostructured n-type semiconductor. Cu_2S (chalcocite), with a band gap of 1.2 eV[9] and an absorption coefficient of 10^5 cm^{-1} at 750 nm,[10] could be an interesting absorber and p-type conductor. Reynolds and co-workers have reported solar energy conversion in a CdS/Cu_2S system as early as 1954.[11] CdS/Cu_2S solar cells have been prepared with energy conversion efficiencies up to 5%,[12] but poor stability of the cell has led to a strong decrease in attention in the late 1980s. Cu_xS is known to have five stable phases at room temperature, ranging from the Cu-rich Cu_2S to the Cu-poor CuS phase.[13] Besides Cu_2S, also $Cu_{1.96}S$ (djurleite) and $Cu_{1.8}S$ (digenite) exhibit photovoltaic activity, even though the electrical conductivities and the indirect band gaps increase for the Cu-poor phases.[9]

A variety of gas-phase techniquies have been applied to deposit Cu_2S thin films, such as single-source evaporation[14−16] and (reactive) sputtering.[17,18] Chemical vapor deposition (CVD) has also been employed, but no single-phase films could be obtained.[19,20] Besides CVD, these techniques are so-called line-of-sight techniques and are not suitable for the deposition of Cu_2S films on highly structured and porous substrates. CVD and atomic layer deposition (ALD) can yield conformal thin films. In CVD, gaseous precursors are fed into the reactor chamber simultaneously, while in ALD, the reactants are applied sequentially. Advantages of these techniques, besides a conformal deposition, are excellent control over the film thickness and high purity of the deposited films. ALD and CVD are both used for the deposition of, e.g., oxide semiconductors,[21,22] superconductors,[23,24] and electroluminescent materials.[25,26]

---

(1) O'Regan, B.; Grätzel, M. *Nature* **1991**, *353*, 737.
(2) Tennakone, K.; Kumara, G. R. R. A.; Kumarasinghe, A. R.; Wijayantha, K. G. U.; Sirimanne, P. M. *Semicond. Sci. Technol.* **1995**, *10*, 1689.
(3) O'Regan, B.; Schwartz, D. T.; Zakeeruddin, S. M.; Grätzel, M. *Adv. Mater.* **2000**, *12*, 1263.
(4) Tennakone, K.; Kumara, G. R. R. A.; Wijayantha, K. G. U.; Kottegoda, I. R. M.; Perera, V. P. S.; Aponsu, G. M. L. P. *Semicond. Sci. Technol.* **1998**, *13*, 134.
(5) Bach,U.; Lupo, D.; Comte, P.; Moser, J. E.; Weissörtel, F.; Salbeck, J.; Spreitzner, H.; Grätzel, M. *Nature* **1998**, *395*, 583.
(6) Ernst,K.; Sieber, I.; Neumann-Spallart, M.; Lux-Steiner, M. C.; Könenkamp, R. *Thin Solid Films* **2000**, *361−362*, 213.
(7) Kaiser, I.; Ernst, K.; Fischer, C.-H.; Könenkamp, R.; Rost, C.; Sieber, I.; Lux-Steiner, M. C. *Sol. Energy Mater. Sol. Cells* **2001**, *67*, 89.
(8) Möller, J.; Fischer, C.-H.; Muffler, H.-J.; Könenkamp, R.; Kaiser, I.; Kelch, C.; Lux-Steiner, M. C. *Thin Solid Films* **2000**, *361−362*, 113.
(9) Nair, M. T. S.; Guerrero, L.; Nair, P. K. *Semicond. Sci. Technol.* **1998**, *13*, 1164.
(10) Hewig, G. H.; Pfisterer, F.; Schock, H. W.; Arndt, W.; Bloss, W. H. *Conf. Rec. IEEE Photovoltaic Spec. Conf.* **1982**, 713.
(11) Reynolds, D. C.; Leies, G.; Antes, L. T.; Marburger, R. E. *Phys. Rev.* **1954**, *96*, 533.
(12) Vanhoecke, E.; Burgelman, M.; Anaf, L. *Thin Solid Films* **1986**, *144*, 223.
(13) Hwang, H. L.; Loferski, J. J.; DeMeo, E. A.; Beaulieu, R. *J. Cryst. Growth* **1982**, *59*, 425.
(14) Llabres, J.; Arjona, F. *Phys. Status Solidi A* **1980**, *58*, 153.
(15) Aperathitis, E.; Bryant, F. J.; Scott, C. G. *Sol. Energy Mater.* **1990**, *20*, 15.
(16) Leon, M.; Terao, N.; Rueda, F. *J. Mater. Sci.* **1984**, *19*, 113.
(17) Iborra, E.; Santamaria, J.; Martil, I.; Gonzalez-Diaz, G.; Sanchez-Quesada, F. *Vacuum* **187**, *37*, 437.
(18) Vanhoecke, E.; Burgelman, M.; Anaf, L. *Thin Solid Films* **1984**, *144*, 233.
(19) Nomura, R.; Miyawaki, K.; Toyosaki, T.; Matsuda, H. *Chem. Vap. Dep.* **1996**, *2*, 174.
(20) Hwang, H. L.; Ho, J. S.; Ou, H. J.; Lee, Y. K.; Sun, C. Y.; Chen, C. J.; Loferski, J. J. *Conf. Rec. IEEE Photovoltaic Spec. Conf.* **1981**, 1035.
(21) O'Neill,S. A.; Clark, R. J. H.; Parkin, I. P.; Elliot, N.; Mills, A. *Chem. Mater.* **2003**, *15*, 46.
(22) Aarik, J.; Aidla, A.; Mandar, H.; Uustare, T.; Shuisky, M.; Harsta, A. *J. Cryst. Growth* **2002**, *242*, 189.

10.1021/cm035238b CCC: $30.25

Elsewhere, we have reported the ALD of Cu_xS, using copper bis-tetramethylheptanedionate, $Cu(thd)_2$, and H_2S as the precursors.[27] Here, we describe the CVD of Cu_xS using the same precursors. It appears that the decomposition of $Cu(thd)_2$ governs the deposition mechanism in both cases. By comparison of ALD and CVD, detailed information on the surface chemistry is obtained.

Experimental Aspects

Cu_xS films are deposited using home-built CVD and ALD reactors. In both cases, $Cu(thd)_2$ (Strem Chemicals) is evaporated in a quartz boat inside the reactor at 117 °C. H_2S (4.8 Hoekloos) is used as the sulfur source in both processes, while H_2 (4.8 Hoekloos) is used as the carrier and bulk gas in the CVD of Cu_xS and N_2 (4.8 Hoekloos) acts as carrier, bulk, and valving gas in the ALD of Cu_xS.

In CVD, Cu_xS films are deposited at temperatures between 125 and 505 °C. The partial pressures of $Cu(thd)_2$ and H_2S are 2 and 0.24 mbar, respectively, while the total pressure is kept constant at 25 mbar. In ALD, the deposition temperature varies between 125 and 280 °C. The precursors are applied sequentially into the reactor. First a $Cu(thd)_2$ pulse of typically 2.5 s is applied, followed by a 1.5-s N_2 purge. Subsequently a 1-s H_2S pulse is applied, again followed by a 1.5-s N_2 purge. Thus, one cycle takes typically 6.5 s. The reactor pressure is kept constant at 2 mbar.

Films are deposited on glass microscope slides (Menzel-Glaser) and Corning 7059 glass substrates, which are cleaned ultrasonically in 1:1:1 ethanol, methanol, and propanol, and subsequently rinsed in distilled water and dried under a N_2 flow. The film thickness of the deposited Cu_xS films is measured using a surface texture profiler (Dektak 3030ST). The morphology of the CVD films has been determined using a scanning electron microscope (JEOL JSM-5800LV), while the morphology of the ALD films has been determined using an atomic force microscope (Digital Instruments nanoscope III). Grazing incidence X-ray diffraction (GI-XRD) measurements (Bruker D8 Advance Diffractometer) have been carried out to identify and characterize the crystalline phases.

Results

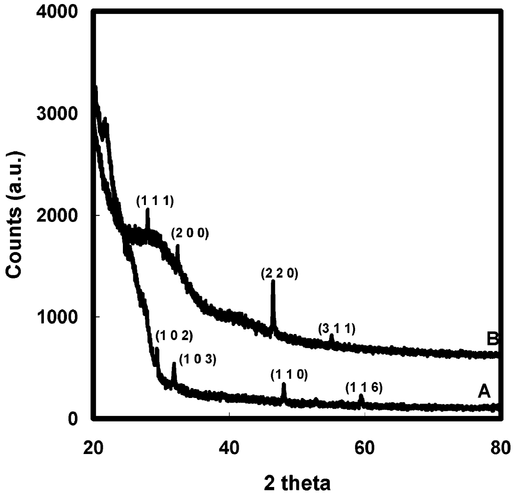

Figure 1. XRD patterns of two ALD grown films. (A) CuS film grown at 150 °C and (B) $Cu_{1.8}S$ film grown at 200 °C.

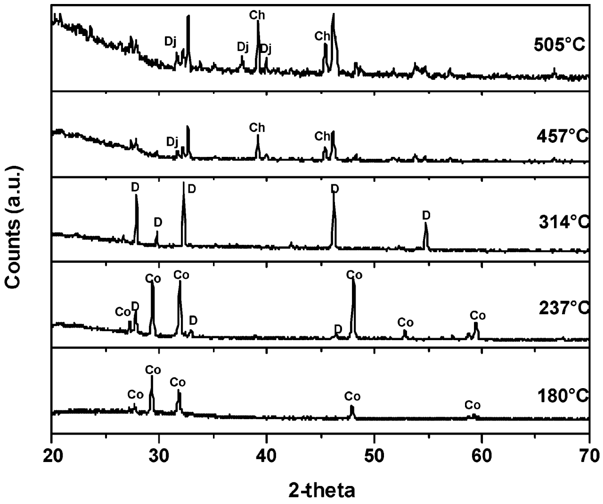

Figure 2. XRD patterns of CVD grown films: Co−CuS (covelitte), D−$Cu_{1.8}S$ (digenite), Dj−$Cu_{1.96}S$ (djurleite), Ch−Cu_2S (chalcocite).

Smooth and well-adhering Cu_xS films can be deposited using $Cu(thd)_2$ and H_2S in both CVD and ALD. The most striking difference between the ALD and CVD processes is that in CVD the presence of H_2 is necessary for growth to occur, while this is not the case in ALD. The reason for this has been explained elsewhere[33] and will be summarized below. We will focus here on the CVD of Cu_xS and repeat relevant details of the ALD process. Subsequently the CVD and ALD processes will be compared and a general decomposition mechanism for $Cu(thd)_2$ is proposed, which explains all major features of both the CVD and the ALD process.

Crystalline Phases. In CVD and in ALD, the crystalline phase depends on the deposition temperature. In both cases, CuS forms at low temperatures. In ALD, a well-defined phase transition from CuS to $Cu_{1.8}S$ is observed at 175 °C, as is shown in Figure 1. Smooth single-phase $Cu_{1.8}S$ films are obtained between 175 and 280 °C, above which the films lose their uniformity and smoothness.

In CVD no sharp phase transitions occur and roughly five different regimes can be distinguished (see Figure 2 and Table 1). Single-phase CuS is grown up to 227 °C. Above this temperature $Cu_{1.8}S$ appears in the films. The $Cu_{1.8}S$ fraction increases with increasing temperature, and at 284 °C, single-phase $Cu_{1.8}S$ is formed. Increasing the temperature above 314 °C yields the formation of fractions of $Cu_{1.96}S$ and Cu_2S in the films.

Growth Rate. Figure 3 shows the growth rate per cycle as a function of temperature for ALD-grown films. Remarkably, the growth rate drops rapidly from 0.4 to 0.2 Å/cycle

---

(23) Dahmen, K. H.; Gerfin, T. *Prog. Cryst. Growth Ch.* **1993**, *2*, 117.
(24) Oda, S.; Zama, H.; Yamamoto, S. *J. Cryst. Growth* **1994**, *145*, 232.
(25) Barth, K. W.; Lau, J. E.; Peterson, G. G.; Endisch, D.; Kaloyeros, A. E.; Tuenge, R. T.; King, C. N. *J. Electrochem. Soc.* **2000**, *147*, 2174.
(26) Ihanus, J.; Hanninen, T.; Hatanpaa, T.; Aaltonen, T.; Mutikainen, I.; Sajavaara, T.; Keinonen, J.; Ritala, M.; Leskelä, M. *Chem. Mater.* **2002**, *14*, 1937.
(27) Reijnen, L.; Meester, B.; Goossens, A.; Schoonman, J. *Chem. Vap. Dep.* **2003**, *9*, 15.
(28) Hanoaka, K.; Ohnishi, H.; Harima, H.; Tachibana, K. *Physica C* **1991**, 145.
(29) Turgambaeva, A. E.; Bykov, A. F.; Igumenov, I. K. *J. Phys. IV* **1995**, C5−221.
(30) Tobaly, P.; Lanchec, G. *J. Chem. Thermodyn.* **1993**, *25*, 503.
(31) Mårtensson, P.; Carlsson, J.-O. *J. Electrochem. Soc.* **1998**, *145*, 2926.
(32) Turgambaeva, A. E.; Bykov, A. F.; Igumenov, I. K. *J. Phys. IV* **1997**, *97−25*, 139.
(33) Reijnen, L.; Meester, B.; Goossens, A.; Schoonman, J., to be published.

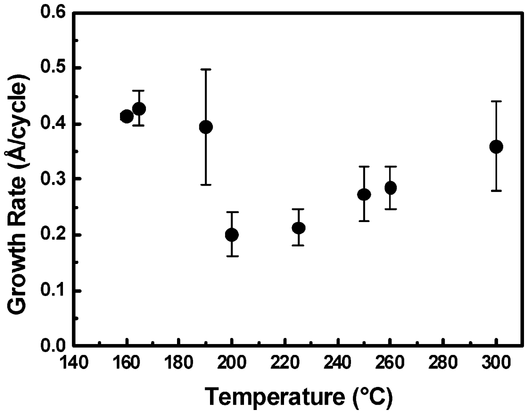

Figure 3. Growth rate per cycle as a function of temperature for ALD-grown Cu_xS films. The vertical bars correspond to the measured standard deviation.

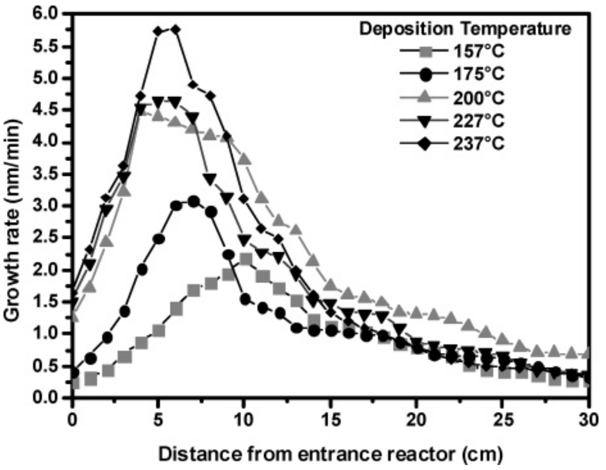

Figure 4. Growth rate as a function of temperature and axial flow axis for CVD-grown Cu_xS films.

Table 1. Dependence of the Crystalline Phases on the Deposition Temperature

temperature	crystalline phase	name
125−227 °C	CuS	covellite
227−284 °C	CuS, $Cu_{1.8}S$	covellite, digenite
284−340 °C	$Cu_{1.8}S$	digenite
340−460 °C	$Cu_{1.8}S$, $Cu_{1.96}S$	digenite, djurleite
460−505 °C	$Cu_{1.8}S$, $Cu_{1.96}S$, Cu_2S	digenite, djurleite, chalcocite

at 190 °C, corresponding to the temperature at which the deposited phase shifts from CuS to $Cu_{1.8}S$. We argued elsewhere[27] that this difference in growth rate of CuS and $Cu_{1.8}S$ is due the fact that only one monolayer of $Cu(thd)_2$ adsorbs per cycle, while $Cu_{1.8}S$ contains almost twice as much copper per unit cell than CuS. The ALD process is not self-limiting at temperatures above 175 °C[27] due to the decomposition of $Cu(thd)_2$, but the growth rate does not increase with the deposition temperature up to about 240 °C. This indicates that up to this temperature decomposition of $Cu(thd)_2$ takes place after adsorption at the surface and that decomposition in the gas phase does not occur.

For CVD films the growth rate as function of temperature and axial flow axis at a $Cu(thd)_2$ partial pressure of 2 mbar and a H_2S partial pressure of 0.24 mbar is shown in Figure 4. It is evident that a pronounced deposition profile is present along the flow axis, which increases with increasing temperature. At temperatures higher than 250 °C the films become too rough for an accurate determination of the growth rate, but the same general deposition profile is present. At these higher temperatures the onset of the deposition shifts toward the entrance of the reactor and the deposition profile becomes less pronounced. It is shown elsewhere[33] that this deposition profile is largely independent of the $Cu(thd)_2$ concentration in the reactor, indicating that depletion of $Cu(thd)_2$ does not occur and that the deposition profile becomes more pronounced when Hthd, a product of the reaction between $Cu(thd)_2$ and H_2S, is added to the reactor. Because of this profile, the activation energy for the deposition reaction cannot be obtained.

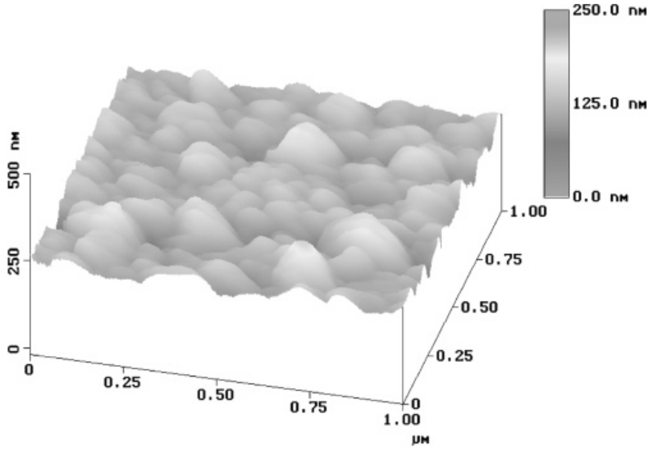

Figure 5. Surface morphology of an ALD-grown $Cu_{1.8}S$ film deposited at 200 °C as determined by AFM.

Morphology. Cu_xS films deposited by ALD are smooth and uniform. The local thickness varies around 9% over the 5 × 5 cm^2 substrate in the roughest films. Figure 5 shows an atomic force microscopy (AFM) image of a 30 nm thick $Cu_{1.8}S$ film grown at 200 °C. The film consists of 100 nm wide grains that grow perpendicular to the substrate surface. The morphology and size of the grains are independent of the deposition parameters.

In contrast, the morphology of CVD films depends strongly on the deposition temperature. Between 125 and 280 °C, well-adhering films with a fine-grained structure are deposited. Films are smooth, but the surface roughness is significantly higher than that of ALD films. The size of the grains increases with increasing temperature from an average of 0.36 μm at 175 °C to an average of 1.15 μm at 248 °C. Increasing the deposition temperature beyond 250 °C results in the deposition of rough films with different grain sizes randomly distributed across the surface (see Figure 6).

Discussion

Several remarkable features of the ALD and CVD processes and differences between them are observed, i.e., the CuS to $Cu_{1.8}S$ phase transition is sharp in ALD and gradual in CVD with a 52 °C higher onset temperature. A pronounced deposition profile is present in CVD, while this profile is absent in ALD up to 280 °C. The morphology in CVD depends on the temperature, while this is not the case in ALD. All these features can be explained by the thermal decomposition of $Cu(thd)_2$, as will be discussed below. The thermal decomposition of $Cu(thd)_2$ in inert gas has been discussed previously[27] and the main conclusions of that

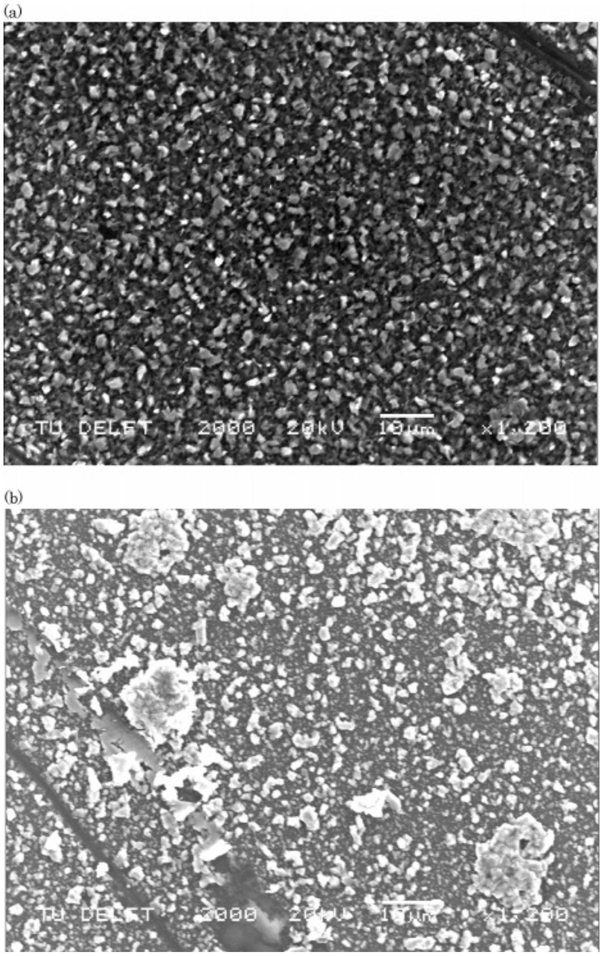

Figure 6. Surface morphology of a smooth CVD-grown CuS/Cu$_{1.8}$S film deposited at 248 °C (a) and of a rough Cu$_x$S film deposited at 505 °C (b) as determined by scanning electron microscopy.

discussion are summarized here. Two different onset temperatures for the decomposition of Cu(thd)$_2$ are reported in the literature: Hanaoka et al.[28] and Turgambaeva et al.[29] report a decomposition temperature around the boiling point of Cu(thd)$_2$, i.e., ±315 °C, while Tobaly et al.,[30] supported by differential scanning calorimetry experiments performed in our laboratory,[27] arrive at a decomposition temperature in the range of 160−175 °C. Mårtenson et al.[31] argued that the decomposition of Cu(thd)$_2$ starts at 175 °C but is slow up to 300 °C. Our experiments in both the ALD and the CVD process agree with this conclusion. The decomposition of Cu(thd)$_2$ starts with the internal reduction of Cu^{2+} to Cu^{1+} followed by the release of a thd ligand or parts thereof. If no further reactants are present, the decomposition of Cu(thd)$_2$ leads to the deposition of copper oxide.

The CuS to Cu$_{1.8}$S Phase Transition. A remarkable difference between ALD and CVD is the onset of the CuS to Cu$_{1.8}$S phase transition. The reduction of Cu^{2+} to Cu^{1+} upon decomposition of Cu(thd)$_2$ at 175 °C is responsible for the phase transition in ALD. Although the reduction of copper is, logically, also responsible for the phase transition in CVD, the temperature at which this occurs is much higher, 227 °C, and the transition is less sharp. The presence of hydrogen as carrier and bulk gas in CVD and not in ALD could lead to a different decomposition temperature of Cu(thd)$_2$ and, thus, to a different phase transition temperature. Turgambaeva et al.[32] studied the decomposition of a large number of β-diketonates. They found that for metal acetylacetonates the onset temperature of the decomposition increases in a H$_2$ atmosphere as opposed to an inert gas atmosphere. For other β-diketonates, the onset temperature of the decomposition remains approximately the same, or is slightly lower in a H$_2$ ambient. The decomposition of M(thd)$_n$ in H$_2$ is only studied for Ni(thd)$_2$, where the onset of the decomposition temperature decreases about 120 °C compared to the decomposition in an inert atmosphere. To investigate the influence of H$_2$ on the Cu(thd)$_2$ decomposition behavior, an ALD experiment has been performed at 200 °C in which H$_2$ is added to the gas stream. No difference between the Cu$_{1.8}$S films deposited with and without additional H$_2$ is observed. Accordingly, the addition of H$_2$ in CVD cannot explain the increase in the transition temperature from CuS to Cu$_{1.8}$S compared to ALD.

At temperatures above 175 °C, the decomposition of Cu(thd)$_2$ leads to loss of self-limitation in ALD, but because Cu(thd)$_2$ decomposition is slow below 280 °C, smooth and homogeneous films can still be obtained up to this temperature.[27] Since Cu(thd)$_2$ is supplied first in ALD, the decomposition of Cu(thd)$_2$ above 175 °C occurs during this pulse and the subsequent N$_2$ purge. As discussed above, Cu(thd)$_2$ decomposes after adsorption at the surface. The decomposition is then followed by the reaction to Cu$_{1.8}$S during the H$_2$S pulse. Cu(thd)$_2$ has several seconds to decompose, and the phase transition is sharp. In CVD both Cu(thd)$_2$ and H$_2$S are present in the gas phase, and the decomposition of Cu(thd)$_2$ and its reaction with H$_2$S compete. At temperatures between 175 and 227 °C, the decomposition of Cu(thd)$_2$ is slow compared to the reaction between Cu(thd)$_2$ and H$_2$S, and all Cu(thd)$_2$ reacts with H$_2$S to CuS before decomposition occurs. When the temperature is raised, the rate of the Cu(thd)$_2$ decomposition increases stronger than the rate of the reaction between Cu(thd)$_2$ and H$_2$S, leading to a film consisting of both CuS and Cu$_{1.8}$S, in which the Cu$_{1.8}$S content increases with increasing temperature. At 384 °C, all Cu(thd)$_2$ has decomposed before the reaction with H$_2$S occurs, leading to the deposition of single-phase Cu$_{1.8}$S. At even higher temperatures, Cu$_{1.96}$S and Cu$_2$S appear in the CVD films. Because self-limitation in ALD is completely lost at these temperatures, a comparison between CVD and ALD is then meaningless.

The Deposition Profile. The origin of the deposition profile in CVD is discussed in detail elsewhere.[33] There, it is shown that the profile can be explained by surface contamination of the reaction product Hthd, which adsorbs at the surface and blocks active surface sites. Hthd can only be removed from the surface by H$_2$, explaining the necessity of H$_2$ in the CVD of Cu$_x$S. Because Hthd is produced in the reaction and Cu(thd)$_2$ is consumed, the Hthd/Cu(thd)$_2$ ratio increases along the flow axis, which limits the growth further downstream and gives rise to a deposition profile. The increasing growth rate with increasing temperature at the entrance of the reactor (Figure 3) ensures that increasing amounts of Hthd are produced and that the profile becomes more pronounced.

In ALD the presence of H_2 is not necessary, since the precursors are supplied sequentially. Because Hthd is produced during the reaction between $Cu(thd)_2$ and H_2S, it is not present in the reactor chamber during the $Cu(thd)_2$ pulse and does not adsorb competitively. Furthermore, when Hthd is released during the H_2S pulse, all active sites are occupied by $Cu(thd)_2$ and Hthd cannot adsorb.

From the presence of the deposition profile in CVD and its absence in ALD, it can be concluded that $Cu(thd)_2$ must adsorb without decomposition. If $Cu(thd)_2$ would decompose upon adsorption, Hthd would be released and adsorb at the surface and a deposition profile would also be present in ALD.

Morphology. The more pronounced roughness of CVD films compared to that of ALD films is not surprising. The alternating precursor supply in ALD ensures that only self-limiting surface reactions occur and layer-by-layer growth is achieved, giving rise to an excellent uniformity and to a low surface roughness.[34]

In CVD, all precursors are present in the gas phase and smooth films can only be obtained under special circumstances such as a low pressure and temperature, i.e., reaction rate limitation. Because a deposition profile is present, Arrhenius plots cannot be presented. Yet, conclusions about the CVD regime present can still be drawn. The percentage of molecules of $Cu(thd)_2$ that participates in the CVD reaction can be roughly estimated from the growth rate (taking the deposition profile into account), the area of the reactor covered with Cu_xS film, the density of the film, the flow of $Cu(thd)_2$, etc. From this it follows that at 175 °C only 0.077% of $Cu(thd)_2$ molecules participates in the CVD growth. The supersaturation of $Cu(thd)_2$, in combination with the small growth rate (3 nm/min), suggests a relatively fast diffusion of reactants compared to the growth rate leading to a surface reaction controlled regime. Furthermore, numerical simulations[33] show that the $Cu(thd)_2$ concentration is constant throughout the reactor, which again indicates that diffusion is fast compared to the surface reaction. The transition from well-adhering and smooth films to rough and nonuniform films at about 250 °C indicates the transition from a surface reaction controlled regime to a thermodynamic regime. The transition temperature of 250 °C corresponds closely to the temperature at which smooth deposition is lost in ALD, i.e., 280 °C. We conclude that the decomposition of $Cu(thd)_2$ becomes favorable in the gas phase between 250 and 280 °C. This leads to a thermodynamic growth regime in CVD, in which the $Cu(thd)_2$ decomposes in the gas phase and its decomposition products react rapidly with H_2S leading to rough nonuniform films. Apart from the rough morphology, also the decreasing deposition profile at temperatures above 250 °C can be explained. Competitive adsorption between $Cu(thd)_2$ (or its decomposed parts) and Hthd still occurs, but the reaction between $Cu(thd)_2$ and H_2S now also takes place in the gas phase.

In ALD the decomposition of $Cu(thd)_2$ in the gas phase at temperatures over 280 °C leads to continuous growth, because the decomposition products of the $Cu(thd)_2$ do not adsorb self-limiting at the substrate surface. Because of the decomposition of $Cu(thd)_2$, a substantial Hthd concentration is now present in the gas phase during the $Cu(thd)_2$ pulse, leading to competitive adsorption of Hthd and $Cu(thd)_2$ or its decomposition products. Both mechanisms result in the loss of smooth film growth.

Conclusions

Thin films of Cu_xS can be grown by both CVD and ALD using $Cu(thd)_2$ and H_2S as the precursors. Comparison of the CVD process with the ALD process leads to a better understanding of the reaction mechanisms in both processes, as well as a better understanding of the $Cu(thd)_2$ decomposition activation. All major features of the CVD and ALD processes can be explained by the thermal decomposition of $Cu(thd)_2$. In both cases $Cu(thd)_2$ adsorbs at the surface without decomposition for temperatures below 175 °C and reacts subsequently with H_2S. At 175 °C, the onset of the $Cu(thd)_2$ decomposition leads to a phase transition from CuS to $Cu_{1.8}S$ in ALD. The same phase transition in CVD is determined by the decomposition rate of $Cu(thd)_2$ in competition with the rate of the reaction between $Cu(thd)_2$ and H_2S. At temperatures beyond 250 °C homogeneous decomposition of $Cu(thd)_2$ becomes favorable, which leads to a transition from a reaction limited regime to a thermodynamic regime in CVD and loss of film uniformity and homogeneity in ALD.

CM035238B

---

(34) Ritala, M.; Leskelä, M.; Dekker, J. P.; Soininen, P. J.; Skarp, J. *Chem. Vap. Dep.* **1999**, *5*, 7.